

# Range Identification for Perspective Dynamic System with Single Homogeneous Observation

Lili Ma, *Student Member, IEEE*, YangQuan Chen<sup>†</sup> and Kevin L. Moore, *Senior Members, IEEE*

Center for Self-Organizing and Intelligent Systems (CSOIS),

Dept. of Electrical and Computer Engineering, 4160 Old Main Hill,

Utah State University (USU), Logan, UT 84322-4160, USA.

Email: lilima@cc.usu.edu, {yqchen, moorek}@ece.usu.edu

**Abstract**—Perspective problems arise in machine vision when using a camera to observe the scene. Essential problems include identification of unknown states and/or unknown parameters from perspective observations. Range identification is to estimate the states/positions of a moving object with known motion parameters which has been discussed in the literature using nonlinear observers with full homogeneous observations derived from the image plane. In this paper, the same range identification problem is discussed with single homogeneous observation using nonlinear observers. Our simulation results verify the convergence of the observers when their observability conditions are satisfied.

## I. INTRODUCTION

In 3-D motion estimation from image sequences, there are basically two sub-categories of identification problems. One category is to estimate the parameters of the motion dynamics of a moving object. The other is to recover the depth information assuming that the motion parameters are already known. The solutions to the first sub-category of problems can be resolved, to the extent possible, via algorithms such as nonlinear optimization formulations [1], linear least squares/total least squares approximations [2], application of epipolar constraints [3], and nonlinear observers [4], [5], [6]. The second sub-category of problem, which is the main focus of this paper and is referred as range identification problem hereafter, can be solved by nonlinear observers applied to perspective dynamic systems (PDS), which is a class of linear systems with homogeneous observation functions.

With a stationary camera observing a moving object, we assume that the object follows an affine motion described by

$$\begin{bmatrix} \dot{X}(t) \\ \dot{Y}(t) \\ \dot{Z}(t) \end{bmatrix} = \begin{bmatrix} a_{11} & a_{12} & a_{13} \\ a_{21} & a_{22} & a_{23} \\ a_{31} & a_{32} & a_{33} \end{bmatrix} \begin{bmatrix} X(t) \\ Y(t) \\ Z(t) \end{bmatrix} + \begin{bmatrix} b_1 \\ b_2 \\ b_3 \end{bmatrix}. \quad (1)$$

Then, a typical PDS will consist of the above linear dynamic system with the following homogeneous output observations:

$$y_1(t) = \frac{X(t)}{Z(t)}, \quad y_2(t) = \frac{Y(t)}{Z(t)}. \quad (2)$$

At this point, the range identification problem can be described formally in the framework of PDS. That is, assuming that the

motion parameters  $a_{i,j}$  and  $b_i$  for  $i, j = 1, 2, 3$  are known, to estimate the position of an object with an unknown initial condition from observations on the imaging surface [4], [7], [8]. Let

$$y(t) = [y_1(t), y_2(t), y_3(t)]^T = \left[ \frac{X(t)}{Z(t)}, \frac{Y(t)}{Z(t)}, \frac{1}{Z(t)} \right]^T. \quad (3)$$

The derivative of  $y(t)$  is:

$$\begin{cases} \dot{y}_1(t) = a_{13} + (a_{11} - a_{33})y_1 + a_{12}y_2 - a_{31}y_1^2 \\ \quad - a_{32}y_1y_2 + (b_1 - b_3y_1)y_3, \\ \dot{y}_2(t) = a_{23} + a_{21}y_1 + (a_{22} - a_{33})y_2 - a_{31}y_1y_2 \\ \quad - a_{32}y_2^2 + (b_2 - b_3y_2)y_3, \\ \dot{y}_3(t) = -(a_{31}y_1 + a_{32}y_2 + a_{33})y_3 - b_3y_3^2. \end{cases} \quad (4)$$

It is based on the above equivalent nonlinear dynamic system that nonlinear observers have been designed/applied to estimate  $y_3(t)$  from  $y_1(t)$  and  $y_2(t)$ .

Several observers have been designed/applied for the nonlinear dynamics in (4), such as the identifier based observer in [4], the state observer in [7], and the range identification observer in [8], where both  $y_1(t)$  and  $y_2(t)$  are assumed available. In this paper, we consider the range identification problem with single homogeneous observation. That is, when either  $y_1(t)$  or  $y_2(t)$  is known, instead both of them.

The paper is organized as follows. Section II gives a motivation to study the single observation case. In Sec. III, the range identification problem with single observation is carried out via the identifier based observer in [4]. Section IV presents our simulation results and comparisons with the case when both  $y_1(t)$  and  $y_2(t)$  are available. Finally, section V concludes the paper.

## II. MOTIVATION

Existing vision devices typically use a photographic camera or a video camera, in conjunction with an off-the-shelf lens, where a 3-D point is projected onto a plane perpendicular to the camera's optical axis assuming a camera pinhole model. This camera-type projection is a special case of a more general planar imaging surface shown in Fig. 1, where the plane is described by its normal vector  $\vec{n} = [n_1, n_2, n_3]^T$  and a point on the plane, which is assumed to be  $[0, 0, 1]$  for simplicity without loss of generality.

<sup>†</sup> Corresponding author. Tel. (435)797-0148, Fax: (435)797-3054. CSOIS URL: <http://www.csois.usu.edu/>

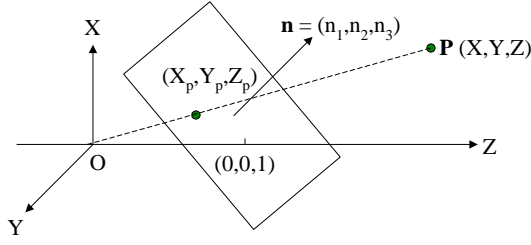


Fig. 1. A general planar imaging surface passing through  $[0, 0, 1]$  with normal vector  $\bar{\mathbf{n}} = [n_1, n_2, n_3]^T$ .

For any point  $[X_p, Y_p, Z_p]^T$  on the general planar imaging surface where the subscript<sub>*p*</sub> denotes the projection, we have

$$n_1 X_p + n_2 Y_p + n_3 (Z_p - 1) = 0, \quad (5)$$

where we further assume that  $n_3 \neq 0$  to emphasize that the observations are somewhat facing toward the  $Z$  axis. Since the projection of a 3-D point  $[X, Y, Z]^T$  can only be observed up to a homogeneous line as

$$X_p = Z_p \frac{X}{Z}, \quad Y_p = Z_p \frac{Y}{Z}, \quad (6)$$

from equations (5) and (6), we have

$$X_p = \frac{n_3 X}{\mathbf{L}_p}, \quad Y_p = \frac{n_3 Y}{\mathbf{L}_p}, \quad Z_p = \frac{n_3 Z}{\mathbf{L}_p}, \quad (7)$$

with  $\mathbf{L}_p \triangleq n_1 X + n_2 Y + n_3 Z$ . Define  $y_g = [y_{g1}, y_{g2}, y_{g3}, y_{g4}]^T$  as

$$y_{g1} = \frac{X}{\mathbf{L}_p}, \quad y_{g2} = \frac{Y}{\mathbf{L}_p}, \quad y_{g3} = \frac{Z}{\mathbf{L}_p}, \quad y_{g4} = \frac{1}{\mathbf{L}_p}. \quad (8)$$

Range identification of a PDS with the general planar imaging surface in Fig. 1 amounts to estimating  $y_{g4}$  using  $(y_{g1}, y_{g2}, y_{g3})$ .

For a conventional camera,  $n_1 = n_2 = 0$  and  $n_3 = 1$ . Equation (8) reduces to

$$y_{g1} = \frac{X}{Z}, \quad y_{g2} = \frac{Y}{Z}, \quad y_{g3} = 1, \quad y_{g4} = \frac{1}{Z}. \quad (9)$$

Compared with (8), equation (4) is already a PDS with partial homogeneous observations due to  $\dot{y}_{g3} = 0$ . Consider a more special situation, as shown in Fig. 2, when an object is moving on a plane  $P_1OP_2$ , whose projection on the image plane is a line  $p_1p_2$  that has either a constant  $y_1(t)$  or a constant  $y_2(t)$ . If  $y_2(t)$  is a constant,  $\dot{y}_2 = 0$ . Range identification problem becomes to identify  $y_2(t)$  and  $y_3(t)$  using  $y_1(t)$ <sup>1</sup>. The above discussion serves as a motivation to investigate the range identification problem for a PDS with single homogeneous observation. However, in the following sections,  $y_2(t)$  will be treated as unavailable, not necessarily be restricted as a constant.

<sup>1</sup>The case to estimate  $y_1(t)$  and  $y_3(t)$  with  $y_2(t)$  is similar

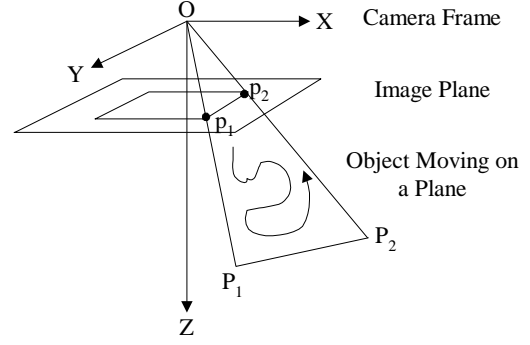


Fig. 2. Illustration of PDS with single observation function.

### III. NONLINEAR OBSERVERS FOR PDS WITH SINGLE HOMOGENEOUS OBSERVATION

Range identification for a PDS using  $(y_1(t)$  and  $y_2(t))$  has been discussed in the literature using the following nonlinear observers:

- 1) The identifier based observer (IBO) proposed in [4] that is motivated from the adaptive control theory and is suitable for the following class of nonlinear systems:

$$\begin{cases} \dot{x}_1 = w^T(x_1, u)x_2 + \phi(x_1, u), \\ \dot{x}_2 = g(x_1, x_2, u), \\ y = x_1, \end{cases} \quad (10)$$

where the matrix  $w^T(x_1, u)$  and the vector  $g(x_1, x_2, u)$  are in general nonlinear functions of their parameters.

- 2) The state observer (SMO) in [7], which is a combination of the sliding mode control method, the adaptive method, and the discontinuous observer techniques.
- 3) The range identification observer (RIO) in [8], which facilitates Lyapunov-based analysis and is motivated from the recent disturbance observer results [9].

In the case of single homogeneous observation using only  $y_1(t)$ , range identification can be solved by a direct application of IBO since the IBO observer is designed for a class of nonlinear systems in the form of (10). Further, based on a resemblance in the constructions of IBO and SMO for the case of full homogeneous observations (when both  $y_1(t)$  and  $y_2(t)$  are available), a modified SMO can be used for the single observation case. However, extension/modification of the RIO observer for the single observation case, though possible, is not straightforward and will not be pursued in this paper.

#### A. Direct Application of IBO

Range identification with single homogeneous observation can be solved by a direct application of the IBO observer, which has been applied to estimate  $y_3(t)$  in [4] when both  $y_1(t)$  and  $y_2(t)$  are available. For the class of nonlinear

systems in (10), the constructed IBO is of the form

$$\begin{cases} \dot{\hat{x}}_1 = GA(\hat{x}_1 - x_1) + w^T(x_1, u)\hat{x}_2 + \phi(x_1, u), \\ \dot{\hat{x}}_2 = -G^2 w(x_1, u)P(\hat{x}_1 - x_1) + g(x_1, \hat{x}_2, u), \\ \hat{x}(t_i^+) = M \frac{\hat{x}(t_i^-)}{\|\hat{x}(t_i^-)\|}, \end{cases} \quad (11)$$

where the sequences of  $t_i$  is defined via

$$t_i = \min \{t : t > t_{i-1} \text{ and } \|\hat{x}(t)\| \geq \gamma M\}, \quad (12)$$

and the matrix  $P$  is a positive definite solution of the Lyapunov equation  $A^T P + PA = -Q$ . In (12),  $M$  is an assumed upper bound for the state estimate  $\|\hat{x}(t)\|$  and  $\gamma$  is a fixed constant with  $\gamma > 1$ . The  $G$  in (11) is a constant scalar gain.

The dynamic system (4) can be rewritten in the form of (10) as

$$\begin{cases} \begin{bmatrix} \dot{y}_1 \\ \dot{y}_2 \end{bmatrix} = \underbrace{\begin{bmatrix} b_1 - b_3 y_1 \\ b_2 - b_3 y_2 \end{bmatrix}}_{w^T([y_1, y_2]^T)} y_3 \\ + \underbrace{\begin{bmatrix} a_{13} + (a_{11} - a_{33})y_1 + a_{12}y_2 - a_{31}y_1^2 - a_{32}y_1y_2 \\ a_{23} + a_{21}y_1 + (a_{22} - a_{33})y_2 - a_{31}y_1y_2 - a_{32}y_2^2 \end{bmatrix}}_{\phi([y_1, y_2]^T)}, \\ \dot{y}_3 = \underbrace{-(a_{31}y_1 + a_{32}y_2 + a_{33})y_3 - b_3 y_3^2}_{g([y_1, y_2]^T, y_3)}, \end{cases} \quad (13)$$

and

$$\begin{cases} \dot{y}_1 = \underbrace{\begin{bmatrix} a_{12} - a_{32}y_1, & b_1 - b_3 y_1 \end{bmatrix}}_{w^T(y_1)} \begin{bmatrix} y_2 \\ y_3 \end{bmatrix} \\ + \underbrace{\begin{bmatrix} a_{13} + (a_{11} - a_{33})y_1 - a_{31}y_1^2 \\ a_{23} + a_{21}y_1 + (a_{22} - a_{33})y_2 - a_{31}y_1y_2 - a_{32}y_2^2 \end{bmatrix}}_{\phi(y_1)}, \\ \begin{bmatrix} \dot{y}_2 \\ \dot{y}_3 \end{bmatrix} = \underbrace{\begin{bmatrix} \text{Same as } \dot{y}_2 \text{ in (4)} \\ \text{Same as } \dot{y}_3 \text{ in (4)} \end{bmatrix}}_{g(y_1, [y_2, y_3]^T)}, \end{cases} \quad (14)$$

respectively. Define

$$e_1 = y_1 - \hat{y}_1, \quad e_2 = y_2 - \hat{y}_2, \quad e_3 = y_3 - \hat{y}_3. \quad (15)$$

The constructed IBO observers for the case when  $(y_1(t), y_2(t))$  are available and when only  $y_1(t)$  is available take the following forms:

$$\text{IBO}_{y_1+y_2} : \begin{cases} \begin{bmatrix} \dot{\hat{y}}_1 \\ \dot{\hat{y}}_2 \end{bmatrix} = GA \begin{bmatrix} e_1 \\ e_2 \end{bmatrix} + \begin{bmatrix} b_1 - b_3 y_1 \\ b_2 - b_3 y_2 \end{bmatrix} \hat{y}_3 \\ + \begin{bmatrix} a_{13} + (a_{11} - a_{33})y_1 + a_{12}y_2 \\ a_{23} + a_{21}y_1 + (a_{22} - a_{33})y_2 \end{bmatrix} \\ - \begin{bmatrix} a_{31}y_1^2 + a_{32}y_1y_2 \\ a_{31}y_1y_2 + a_{32}y_2^2 \end{bmatrix}, \\ \dot{\hat{y}}_3 = -G^2 \begin{bmatrix} b_1 - b_3 y_1 & b_2 - b_3 y_2 \end{bmatrix} P \begin{bmatrix} e_1 \\ e_2 \end{bmatrix} \\ - (a_{31}y_1 + a_{32}y_2 + a_{33})\hat{y}_3 - b_3 \hat{y}_3^2, \end{cases} \quad (16)$$

and

$$\text{IBO}_{y_1} : \begin{cases} \dot{\hat{y}}_1 = GA e_1 + [a_{12} - a_{32}y_1, b_1 - b_3 y_1] \begin{bmatrix} \hat{y}_2 \\ \hat{y}_3 \end{bmatrix} \\ + [a_{13} + (a_{11} - a_{33})y_1 - a_{31}y_1^2], \\ \begin{bmatrix} \dot{\hat{y}}_2 \\ \dot{\hat{y}}_3 \end{bmatrix} = -G^2 \begin{bmatrix} a_{12} - a_{32}y_1 \\ b_1 - b_3 y_1 \end{bmatrix} P e_1 \\ + \begin{bmatrix} a_{23} + a_{21}y_1 + (a_{22} - a_{33})\hat{y}_2 \\ -(a_{31}y_1 + a_{32}\hat{y}_2 + a_{33})\hat{y}_3 \end{bmatrix} \\ + \begin{bmatrix} -a_{31}y_1\hat{y}_2 - a_{32}\hat{y}_2^2 + (b_2 - b_3\hat{y}_2)\hat{y}_3 \\ -b_3\hat{y}_3^2 \end{bmatrix}, \end{cases} \quad (17)$$

under the corresponding observability conditions

$$\lambda_{\min}\{w([y_1(t), y_2(t)]^T) w^T([y_1(t), y_2(t)]^T)\} > \varepsilon > 0, \quad (18)$$

and

$$\lambda_{\min}\{w(y_1(t)) w^T(y_1(t))\} > \varepsilon > 0, \quad (19)$$

where  $\lambda_{\min}$  denotes the smallest eigenvalue of a matrix. Notationwise, all the observer parameters correspond to their specific observers, i.e.,  $G$  or  $\gamma$  do not share a global meaning.

The two observability conditions in (18) and (19) are of the same level of complexity. Substituting  $w^T([y_1, y_2]^T) = [b_1 - b_3 y_1, b_2 - b_3 y_2]^T$  and  $w^T(y_1) = [a_{12} - a_{32}y_1, b_1 - b_3 y_1]$  into (18) and (19), we have

$$\lambda_{\min}\{(b_1 - b_3 y_1)^2 + (b_2 - b_3 y_2)^2\} > 0, \quad (20)$$

and

$$\lambda_{\min}\left\{\begin{bmatrix} \tilde{a}^2 & \tilde{a}\tilde{b} \\ \tilde{a}\tilde{b} & \tilde{b}^2 \end{bmatrix}\right\} > 0, \quad (21)$$

with  $\tilde{a} = a_{12} - a_{32}y_1$  and  $\tilde{b} = b_1 - b_3 y_1$ . The above two conditions are equivalent to

$$(b_1 - b_3 y_1)^2 + (b_2 - b_3 y_2)^2 > 0, \quad (22)$$

and

$$(b_1 - b_3 y_1)^2 + (a_{12} - a_{32}y_1)^2 > 0, \quad (23)$$

which are obviously of the same complexity.

Proof of IBO <sub>$y_1$</sub> , the observer in (17) for the single homogeneous observation case, is omitted from here since it is a direct application of the IBO, with its detailed proof provided in [4].

### B. Direct Modification of SMO

The SMO observer proposed in [7] has been applied to the state estimation of (4) when both  $y_1(t)$  and  $y_2(t)$  are available. When only  $y_1(t)$  is available, the following observer, which is based on a modification of the SMO and a resemblance between SMO and IBO, can also be used for the state

estimation of  $y_2(t)$  and  $y_3(t)$ :

$$\text{SMO}_{y_1} : \begin{cases} \dot{\hat{y}}_1 = \frac{\hat{\lambda}_1(t)e_1}{|e_1| + \delta_1} + [a_{12} - a_{32}y_1, b_1 - b_3y_1] \begin{bmatrix} \hat{y}_2 \\ \hat{y}_3 \end{bmatrix} \\ \quad + [a_{13} + (a_{11} - a_{33})y_1 - a_{31}y_1^2], \\ \begin{bmatrix} \dot{\hat{y}}_2 \\ \dot{\hat{y}}_3 \end{bmatrix} = \alpha \begin{bmatrix} a_{12} - a_{32}y_1 \\ b_1 - b_3y_1 \end{bmatrix} \frac{\hat{\lambda}_1(t)e_1}{|e_1| + \delta_1} \\ \quad + \begin{bmatrix} a_{23} + a_{21}y_1 + (a_{22} - a_{33})\hat{y}_2 \\ -(a_{31}y_1 + a_{32}\hat{y}_2 + a_{33})\hat{y}_3 \end{bmatrix} \\ \quad + \begin{bmatrix} -a_{31}y_1\hat{y}_2 - a_{32}\hat{y}_2^2 + (b_2 - b_3\hat{y}_2)\hat{y}_3 \\ -b_3\hat{y}_3^2 \end{bmatrix}, \end{cases} \quad (24)$$

where  $\hat{\lambda}_1(t)$  is adaptively updated by

$$\hat{\lambda}_1(t) = \begin{cases} 2\alpha_1|e_1|, & \text{if } |e_1| > 2\delta_1, \\ 0, & \text{otherwise,} \end{cases} \quad (25)$$

with observability condition similar to that in (19).

The modified SMO observer  $\text{SMO}_{y_1}$  in (24) achieves extremely similar performance to  $\text{IBO}_{y_1}$  using properly chosen observer parameters. However, its proof of convergence is not as straightforward.

#### IV. SIMULATION RESULTS

The range identification observers  $\text{IBO}_{y_1}$  and  $\text{SMO}_{y_1}$  in (17) and (24) for single homogeneous observation are tested via Matlab simulations using the first example in [7], where the target is moving according to the following affine motion:

$$\begin{bmatrix} \dot{X}(t) \\ \dot{Y}(t) \\ \dot{Z}(t) \end{bmatrix} = \begin{bmatrix} -0.2 & 0.4 & -0.6 \\ 0.1 & -0.2 & 0.3 \\ 0.3 & -0.4 & 0.4 \end{bmatrix} \begin{bmatrix} X(t) \\ Y(t) \\ Z(t) \end{bmatrix} + \begin{bmatrix} 0.5 \\ 0.25 \\ 0.3 \end{bmatrix},$$

$$[X(0) \ Y(0) \ Z(0)]^T = [1 \ 1.5 \ 2.5]^T. \quad (26)$$

In our simulations, the observer parameters are chosen to be

$$G = 10, A = 1, P = -1/2, M = 10, \gamma = 1, \quad (27)$$

and

$$\alpha = 5, \hat{\lambda}_1(0) = 1, \alpha_1 = 10, \delta_1 = 0.2, M = 10, \gamma = 1, \quad (28)$$

for the  $\text{IBO}_{y_1}$  and  $\text{SMO}_{y_1}$ , respectively, with initial conditions

$$\begin{aligned} \hat{y}_1(0) &= y_1(0) = X(0)/Z(0) = 0.4, \\ [\hat{y}_2(0), \hat{y}_3(0)] &\in \{[-1, -1], [0, 0], [1, 1]\}. \end{aligned} \quad (29)$$

Since the  $\text{SMO}_{y_1}$  has an extremely close performance to that of  $\text{IBO}_{y_1}$ , simulation results are only presented for the  $\text{IBO}_{y_1}$ .

First, simulation results are presented in Figs. 3, 4, and 5 for  $\text{IBO}_{y_1}$  with the observer parameters (27) and initial conditions (29) in the ideal case with no noise. After 15 seconds, the estimations of  $y_2(t)$  and  $y_3(t)$  converge to their true values.

Next, comparison between  $\text{IBO}_{y_1+y_2}$  and  $\text{IBO}_{y_1}$ , the observers in (16) and (17), in the case of full and single observations is shown in Fig. 6 for the ideal case of no noise with initial

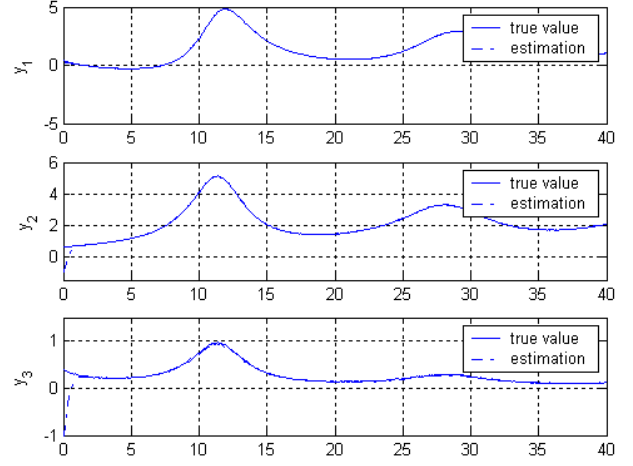


Fig. 3. State estimation using IBO with  $[\hat{y}_2(0), \hat{y}_3(0)] = [-1, -1]$ .

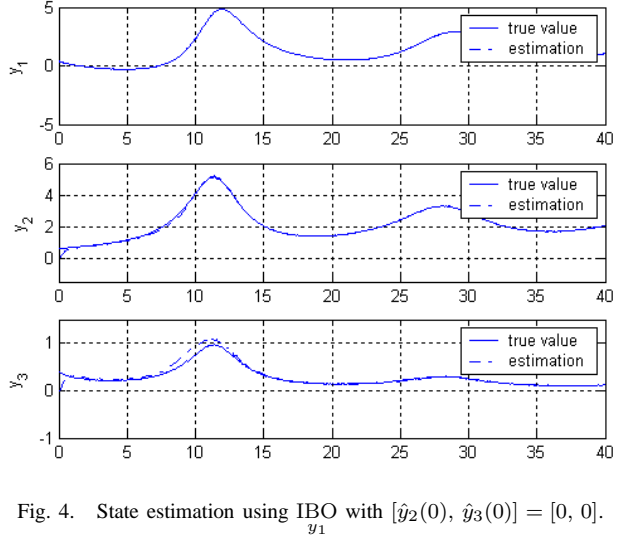


Fig. 4. State estimation using IBO with  $[\hat{y}_2(0), \hat{y}_3(0)] = [0, 0]$ .

conditions  $[\hat{y}_1(0), \hat{y}_2(0), \hat{y}_3(0)] = [0, 0, 0]$  for full observations and  $[\hat{y}_1(0), \hat{y}_2(0), \hat{y}_3(0)] = [X(0)/Z(0), 0, 0]$  for single. It is observed from Fig. 6 that  $\text{IBO}_{y_1}$  for the single case has a less converging speed than that of  $\text{IBO}_{y_1+y_2}$ .

Finally, the observers in  $\text{IBO}_{y_1+y_2}$  and  $\text{IBO}_{y_1}$  are compared for their robustness to noise, where observer performance is shown in Fig. 7 with uniform noise bounded by  $\pm 10^{-2}$ . With a lagging converging performance similar to that in Fig. 6,  $\text{IBO}_{y_1+y_2}$  achieves estimation accuracy comparable to that of  $\text{IBO}_{y_1}$  after 15 seconds. For fair comparison, in the comparisons shown in Figs. 6 and 7, same/similar observer parameters are used:  $M, G, \gamma$  are the same;  $(A, P)$  are chosen to be  $(1, -1/2)$  for  $\text{IBO}_{y_1}$  and  $(I_{2 \times 2}, -I_{2 \times 2}/2)$  for  $\text{IBO}_{y_1+y_2}$ , where  $I_{2 \times 2}$  denotes the identity matrix of dimension 2.

From the above three-step simulation studies, it can be concluded that  $\text{IBO}_{y_1}$ , as well as  $\text{SMO}_{y_1}$ , can achieve satisfactory estimation performance with single observation function. It is

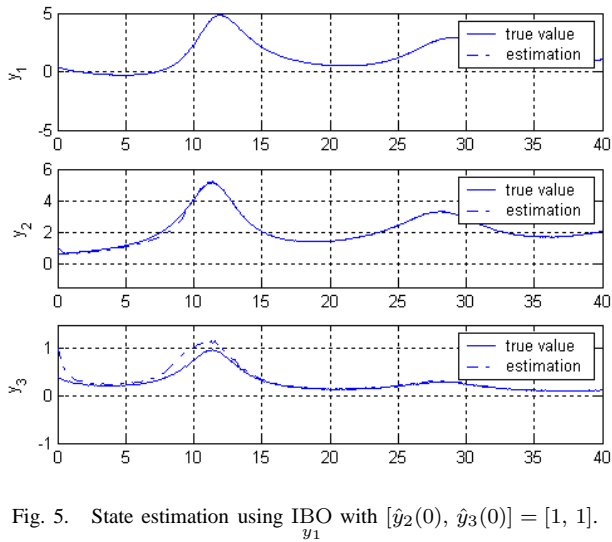


Fig. 5. State estimation using IBO with  $[\hat{y}_2(0), \hat{y}_3(0)] = [1, 1]$ .

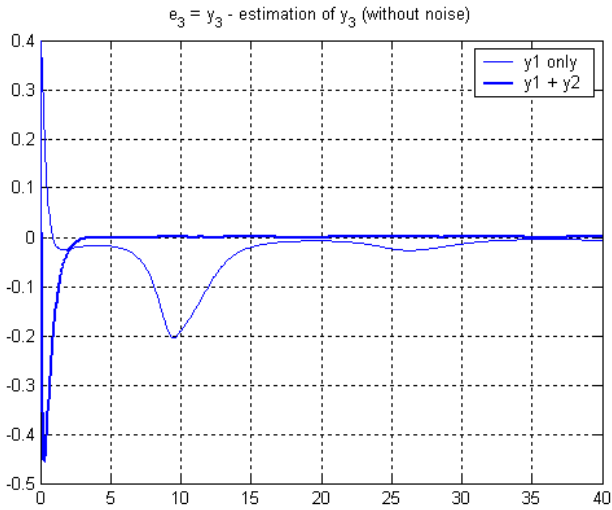


Fig. 6. Estimation error comparison between IBO and IBO in the ideal case of no noise.

unsurprising that their converging speed is not as fast as those with full observations. However, in the presence of noise, the SMO using single homogeneous observation manifests similar robustness performance compared to SMO using full observations.

## V. CONCLUDING REMARKS

For a perspective dynamic system (PDS) with single homogeneous observation function, range identification problem is discussed using nonlinear observers previously used for the full observation case. Our simulation results show that converging speed of the observer for the single observation case is slower than those with full observations. However, both observers have similar robust performance.

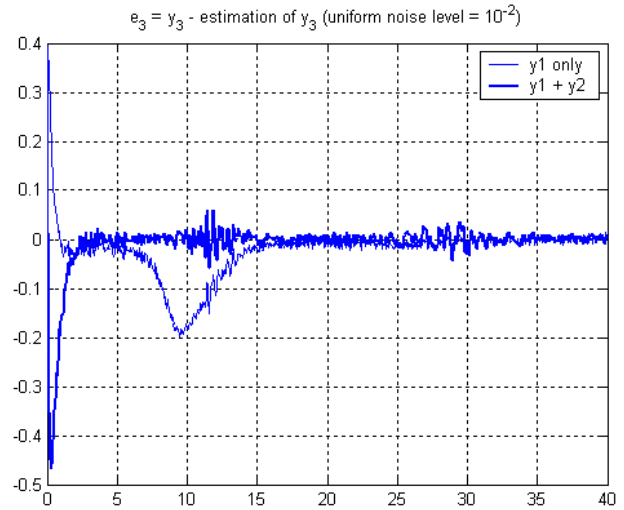


Fig. 7. Estimation error comparison between IBO and IBO in the presence of uniform noise bounded by  $\pm 10^{-2}$ .

## REFERENCES

- [1] H. R. Cho, K. M. Lee, and S. U. Lee, "A new robust 3D motion estimation under perspective projection," in *IEEE Int. Conf. on Image Processing*, 2001, pp. 660–663.
- [2] T. Papadimitriou, K. I. Diamantaras, M. G. Strintzis, and M. Roumeliotis, "Robust estimation of rigid-body 3-D motion parameters based on point correspondences," *IEEE Transactions on Circuits and Systems for Video Technology*, vol. 10, no. 4, pp. 541–549, June 2000.
- [3] S. Soatto, R. Frezza, and P. Perona, "Motion estimation via dynamic vision," *IEEE Transactions on Automatic Control*, vol. 41, no. 3, pp. 393–413, Dec. 1996.
- [4] M. Jankovic and B. K. Ghosh, "Visually guided ranging from observations of points, lines and curves via an identifier based nonlinear observer," *Systems and Control Letters*, vol. 25, pp. 63–73, 1995.
- [5] A. Chiuso, P. Favaro, H. Jin, and S. Soatto, "Structure from motion causally integrated over time," *IEEE Transactions on Pattern Analysis and Machine Intelligence*, vol. 24, no. 4, pp. 523–535, Apr. 2002.
- [6] B. K. Ghosh, M. Jankovic, and Y. T. Wu, "Perspective problems in system theory and its application to machine vision," *Journal of Mathematical Systems, Estimation and Control*, vol. 4, no. 1, pp. 3–38, 1994.
- [7] X. Chen and H. Kano, "A new state observer for perspective systems," *IEEE Transactions on Automatic Control*, vol. 47, no. 4, pp. 658–663, Apr. 2002.
- [8] W. E. D. an Y. Fang, D. M. Dawson, and T. J. Flynn, "Range identification for perspective vision systems," in *Proceedings of the American Control Conf.*, Denver, Colorado, U.S.A, June 4-6 2003, pp. 3448–3453.
- [9] Y. Fang, M. Feemster, D. Dawson, and N. Jalili, "Active interaction force identification for atomic force microscope applications," in *Proceedings of the IEEE Conf. on Decision and Control*, Las Vegas, Nevada, USA, Dec. 2002, pp. 3678–3683.